Nitrogen-induced reconstruction of the $Cu_3Au(110)$ surface

Karina Morgenstern, Matthias Voetz,* and Horst Niehus†
Institut für Grenzflächenforschung und Vakuumphysik, Forschungszentrum Jülich, D-52425 Jülich, Germany
(Received 29 April 1996)

Using low-energy ion backscattering with the detection of neutrals in combination with scanning tunneling microscopy and low-energy electron diffraction, we investigated the $Cu_3Au(110)$ surface upon exposure to nitrogen. Nitrogen was found to induce a Cu-surface segregation and a surface reconstruction to a $c(2\times4)$ pattern. We suggest a model for this reconstruction, which is characterized by additional copper double rows in $\langle 110\rangle$ azimuth with nitrogen atoms in every second bridge position. The nitrogen atoms in neighboring double rows are shifted by one atomic spacing with respect to one another. [S0163-1829(96)01643-8]

I. INTRODUCTION

Metallic alloys are of special interest due to their massive use in catalytic applications. Single crystals of one single atomic species have been intensively investigated with respect to their behavior upon exposure to oxygen and nitrogen. The investigation of binary alloys upon exposure to these gases is a first step toward an understanding of the behavior of more complex, industrially interesting alloys. In this paper, we use neutral impact collision ion-scattering spectroscopy (NICISS), scanning tunneling microscopy (STM), and low-energy electron diffraction (LEED) to investigate the compositional and structural changes occurring at the $Cu_3Au(110)$ surface upon exposure to nitrogen.

In STM images of surfaces of single crystals of one atomic species the electron-density distribution is usually a direct measure of the topography on the surface. The application of the method for mixed systems is, however, less straightforward. In particular, adsorbates may be imaged unexpectedly dependent on the nature of the tip atom.[1–4] In addition, no information of near surface layers can be derived by STM. In contrast, NICISS distinguishes between different atomic species, and is sensitive to more than five surface layers. The combination of the local probe STM method and NICISS, which investigates the averaged local order, has been demonstrated to be a powerful tool for the investigation of surface structures.[5] Here we demonstrate that it is even more powerful for the investigation of binary alloys. In addition, LEED is used to corroborate the long-range order on the reconstructed surface.

II. EXPERIMENT

The STM measurements were carried out in an UHV-chamber described in detail in Ref. 6. The STM is of the Beetle type,[7] and operates at room temperature. For the sample preparation and its control, the chamber contains an ion sputtering gun, electron bombardment heating, a four-grid LEED optic also used as an Auger electron spectrometer (AES), and an infrared pyrometer. The sample is cleaned by ion bombardment with 1 keV Ar^+ ions for 30 min, and subsequent annealing at 773 K for 10 min. The Auger spectrum taken afterwards shows no contaminants. The surface obtained by this procedure, followed by rapidly cooling to room temperature exhibits a (2×1) LEED pattern; in contrast, when the surface is cooled slowly, it exhibits a (4×1) LEED pattern. Both surfaces have been shown to be gold-rich terminated.[8] The saturation coverage of nitrogen as well as its desorption temperature are controlled by the AES. The ion-sputtering gun is also used to dissociate the nitrogen molecules.

Figure 1 shows a STM image of the clean surface in atomic resolution. The rectangle unit cell is indicated. The different atomic species, i.e., copper and gold, are indistinguishable in the STM image. This is in contrast to the case of the $Cu_3Au(100)$ surface, where the different species are distinguishable.[9] Most probably the different contrast on the (100) surface is due to the different relaxation in the topmost layer for the copper and gold atoms, respectively.[10] This leads to the height difference imaged on the (100) surface. The calculated height difference between the Au and Cu atoms is 0.07 Å for the (110) surface, only about half of that for the (100) surface. This most probably causes the nondistinguishability of the two species in Fig. 1.

The UHV chamber used for surface characterization by NICISS was described in detail elsewhere.[5] It has analogous

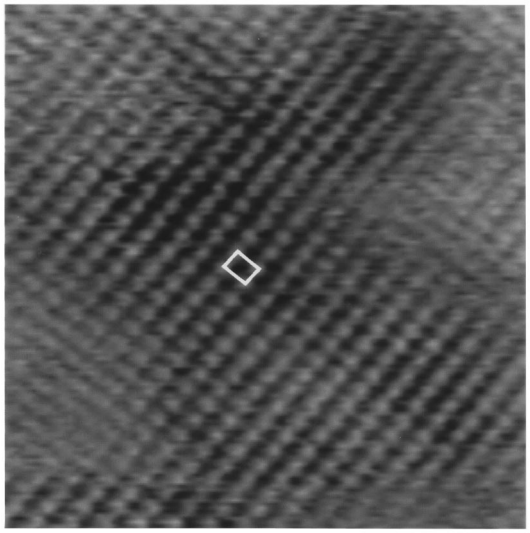

FIG. 1. STM image of the clean $Cu_3Au(110)$ surface in atomic resolution; a unit cell is indicated; $U=0.6$ V, $I=1$ nA, 6.8×6.8 nm^2.

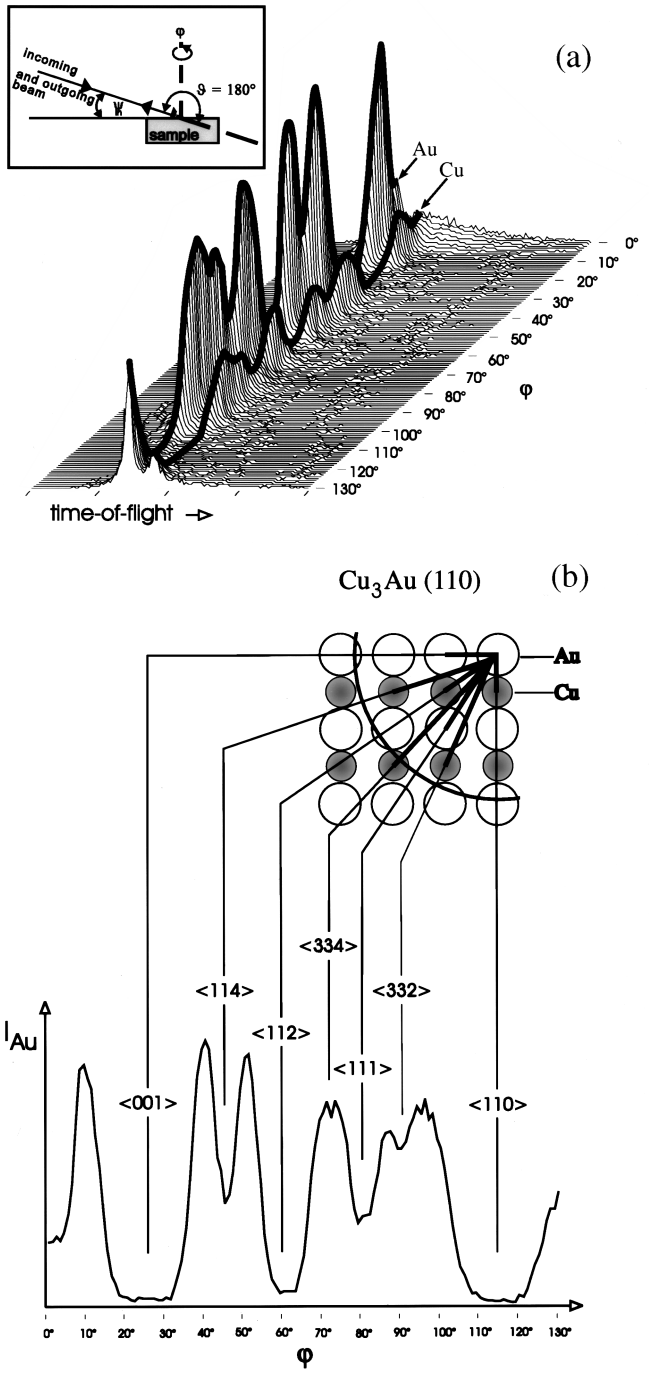

FIG. 2. (a) TOF spectra of the clean $Cu_3Au(110)$ surface; incidence angle $\Psi_{in}=4°$. Black lines indicate the gold and copper φ scans, respectively. The inset shows the used scattering geometry. (b) Gold φ scan for $\Psi_{in}=4°$. Each minimum is related to an azimuthal direction in the surface with a short nearest-neighbor distance as indicated by the black bars in the surface model of the gold-rich terminated surface. The circle segment in the surface model indicates the region where the shadow cone is active for $E_{in}=3.1$ keV.

facilities for ion bombardment, heating, AES, and LEED to those of the STM chamber, which allows a similar sample preparation. The He^+-ion beam of 3.1 keV for the NICISS is produced in a differentially pumped ion gun. A condenser deviates the beam, so that its direction of incidence coincides with the detector direction. This allows a ''real'' 180° NICISS that simplifies the data interpretation considerably. The scattering geometry used is shown in the inset in Fig. 2(a). The fixed scattering angle is $\vartheta=180°$. By varying the azimuthal angle over a span of more than 90° at a fixed glancing incidence angle, a so-called azimuthal scan is obtained. A polar scan is obtained by varying the incidence angle Ψ_{in} from 0° to more than 90° at a fixed azimuthal angle determined beforehand to have a minimum in an azimuthal scan. Such a minimum is caused by a short distance between neighboring atoms in the top surface layer, allowing no backscattering. In the case of the clean surface, short distances are low-indexed azimuths. The energy distribution of of the scattered neutrals is determined by the measurement of TOF (time of flight). The TOF technique is especially suited to an investigation of alloys because it allows the identification of the mass of the surface atoms. Using helium as a probe, all masses except hydrogen and helium can be detected in one spectrum. Here the TOF detector allows us to measure the particles scattered at the surface Au or Cu atoms simultaneously on different channels. Figure 2(a) shows TOF spectra taken on the clean surface at a fixed polar angle of $\Psi_{in}=4°$ and at different azimuthal angles ϕ. Each of the TOF spectra exhibits two maxima which correspond to particles that were scattered on gold and on copper atoms, respectively. Essential structural information can be obtained from the ϕ dependence of the maxima in the TOF spectra associated with scattering from one of the species at the surface as indicated by the black lines in Fig. 2(a). Further plots will therefore show this fraction of the complete TOF scans only.

The ϕ scan for gold, that was used to identify the azimuthal directions, is shown in Fig. 2(b). Each of the minima can be attributed to a short distance between neighboring atoms in the topmost layer of the surface. The model in Fig. 2(b) indicates these by the thick lines. The outlined gold atom acts as the so-called scattering atom. If an ion coincides with $E_{in}=3.1$ keV and $\Psi_{in}=4°$ onto the scattering atom it cannot reach any of the atoms within the circle, and therefore cannot be backscattered. Each of the atoms within the circle therefore causes a minimum in the azimuthal direction indicated. The minima of the Cu φ scan (not shown explicitly) are found at the same angles.

The difficulty to adsorb atomic nitrogen directly from N_2 gas interaction with metal surfaces at room temperature has already been noted for other surfaces [Ni(110),[11] Cu(110),[12] and $Cu_3Au(100)$ (Ref. 9)]. It has been explained by the high dissociation energy of nitrogen molecules. On a $Cu_3Au(110)$ surface exposed to molecular nitrogen at a pressure of 3.5×10^{-5} Torr, no AES-detectable nitrogen adsorbs over several hours. We therefore use nitrogen ion implantation to obtain eventually an adsorbed N-atom layer. The implantation is carried out with the sample facing the gun, and at an acceleration voltage of $U=300$ V (the ion flux is 0.1 A/cm^2). The time needed for implantation of a saturation coverage was determined by AES to be 8 min. An annealing step to a temperature just below the nitrogen desorption temperature caused surface segregation of the nitrogen implanted into deeper layers to the surface. On the Cu(110) surface, a nitrogen reconstruction was induced by an analogous sample preparation.[13] This step was also controlled by

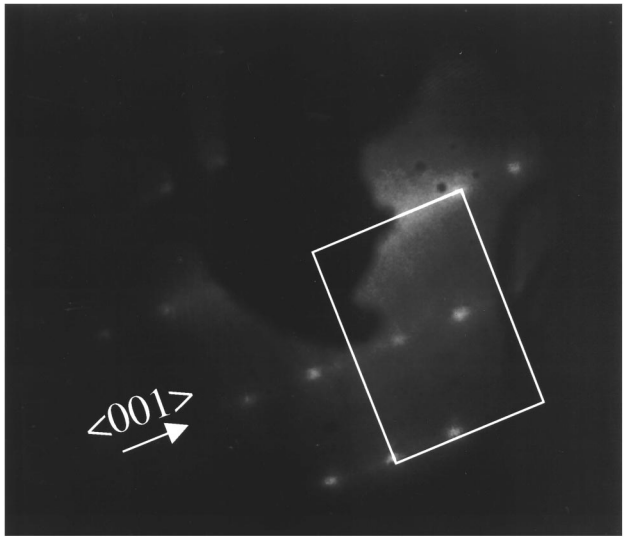

FIG. 3. LEED image of the nitrogen-covered $Cu_3Au(110)$ surface exhibiting a $c(2\times4)$ superstructure. The rectangle indicates the (00), (01), (10), and (11) spots. The (00) spot is covered by the sample.

AES. In contrast to the case with oxygen adsorption of the same surface,[14] the final structure after N exposure and annealing is similar for both the (2×1) and (4×1) structures of the clean surface.

III. RESULTS AND DISCUSSION

A. LEED pattern

Figure 3 shows a LEED image of the nitrogen-covered $Cu_3Au(110)$ surface. It exhibits a $c(2\times4)$ superstructure. The weak LEED reflexes even after annealing can be explained by the roughness caused by the nitrogen implantation. This partial disorder of the topmost layers can also be concluded from the less steep slopes in the NICISS spectra (see below).

B. Nitrogen-induced Cu segregation

In order to estimate the surface composition from the measured NICISS TOF intensities, one can use the formula[15]

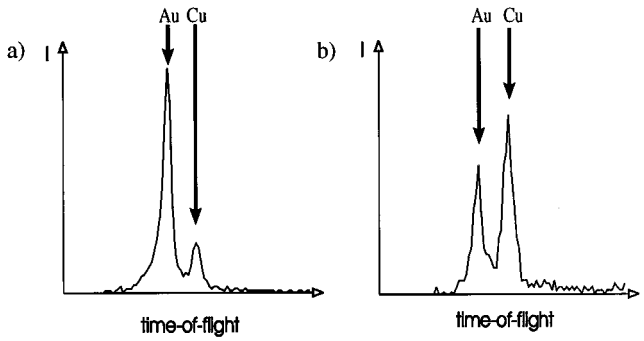

FIG. 4. TOF spectra for $\Psi_{in}=4°$, not low indexed azimuth $\varphi=20°$. (a) Clean $Cu_3Au(110)$ surface. (b) Nitrogen-covered $Cu_3Au(110)$ surface.

$$\frac{N_1}{N_2}=\frac{I_1}{I_2}\left(\frac{Z_2}{Z_1}\right)^2\frac{S_1}{S_2} \tag{1}$$

for the relative fraction of two species in the surface, where N_i is the number of scattering atoms in the irradiated spot, I_i is the measured intensity, Z_i is the atomic number, and S_i takes into account the effect of the shadow cone, i.e., the probability of being reached by the incoming ion beam.[16] Equation (1) is valid for glancing incidence angles for ion/neutral trajectories far away from the shadow cone edge. This is the case in azimuths that exhibit no minimum in a polar scan.

The TOF spectra shown in Fig. 4 are taken at $\Psi_{in}=4°$, and the arbitrary azimuth $\varphi=20°$ before and after nitrogen implantation. They reveal a change in the intensity fraction from $I_{Cu}:I_{Au}=0.23:1$ to $I_{Cu}:I_{Au}=1.43:1$. According to Eq. (1), this is due to a change in the atomic ratio from $N_{Cu}:N_{Au}=1.7:1$ to $N_{Cu}:N_{Au}=11.0:1$, by a factor of more than 6. In other azimuths similar changes have been observed. This is comparable to the induced segregation found upon gas exposure on other surfaces of Cu_3Au. For instance, copper segregation as a result of nitrogen coverage has been detected for $Cu_3Au(100)$.[9] Similarly, Cu segregation was reported for $Au_{0.7}Cu_{0.3}(100)$,[17] for $Au_3Cu(001)$,[18] and for $Cu_3Au(110)$ (Ref. 14) upon oxygen exposure.

C. STM data

Figure 5 shows STM images taken after the exposure to nitrogen and annealing. The similarities with STM data measured at the nitrogen-covered Cu(110) surface are remarkable.[5] As dominating structure elements, on the nitrogen-covered (2×3)-reconstructed Cu(110) surface, copper double rows were seen.[12,19] This reconstruction has been described as a missing row structure with every third $\langle110\rangle$ row missing, wherein nitrogen atoms show a characteristic long-range order. They are proposed to be located at every second bridge position along the $\langle110\rangle$ direction, and aligned in the $\langle001\rangle$ direction.

Figure 5(a) shows the N reconstructed Cu_3Au surface: double rows with dark spots in the $\langle110\rangle$ azimuth can clearly be recognized. At a low nitrogen coverage the double rows build a local (2×3) structure. At saturation coverage the double rows become adjacent [Fig. 5(b)]. Zooming in, Fig. 5(c) shows in atomic resolution that in the $\langle110\rangle$ azimuth the bright spots are 5.6 Å apart, i.e., about two atomic spacings (5.3 Å). In adjacent double rows the spots are displaced by one atomic spacing with respect to the next double row. The distances in and between the double rows measured from the STM images are $a=3.3$ Å and $b=3.9$ Å . We assume that the bright spots are copper atoms, and the dark spots are nitrogen atoms. This assumption is in line with the copper segregation discussed above. In $\langle110\rangle$ azimuth only every second copper atom is visible due to the changes in the electronic structure induced by the nitrogen atoms. STM being mostly insensitive to chemical contrast, it is not possible to prove that the extrema in the electronic corrugation seen in the STM images correspond to the atomic centers. In the following, we will explain the origin of the extrema in the electronic structure imaged by STM based on data of the mass-sensitive technique NICISS, and derive the positions of the atomic cores.

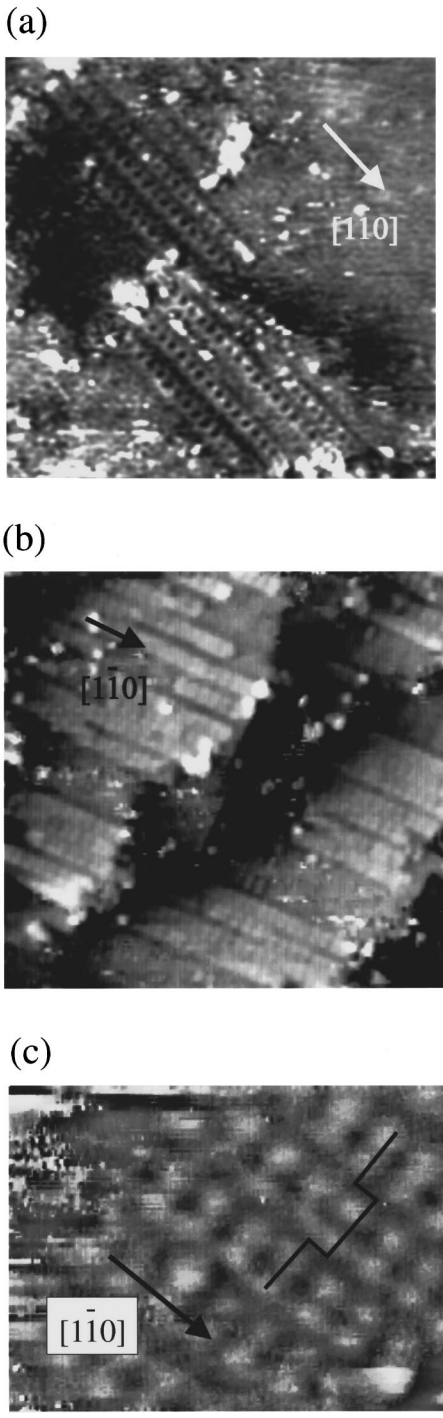

FIG. 5. STM images of the $c(2\times4)$ N-reconstructed $Cu_3Au(110)$ surface exhibiting Cu-N double rows. (a) 157×152 Å ^{2}; $U=0.16$ V; $I=7$ nA. (b) 190×173 Å ^{2}; $U=0.1$ V; $I=1$ nA. (c) Atomic resolution image; the displacement between the rows is indicated; 44×29 Å , $U=1$ V, and $I=1$ nA.

D. Model of the surface structure

We have thus far established that, under the influence of nitrogen, a $c(2\times4)$ reconstruction develops on top of the gold-rich (110) surface that is mainly due to additional copper. The STM images show aligned double rows of bright spots, with dark spots located in the middle of each double row. These dark spots are displaced by one atomic spacing in neighboring double rows. Based on these results of the Secs. III A–III C, we propose a model of the surface as schematically shown in Fig. 6. The model consists of neighboring copper double rows on top of the gold-rich surface. The copper atoms are not exactly positioned above the copper atom of the bulk's second layer: in the $\langle001\rangle$ direction the copper distance (b) between the rows in larger than the distance (a) within the double rows (in-plane relaxation); a kind of ''pairing row.'' Every second of the twofold-coordinated bridge positions of these copper rows is occupied by a nitrogen atom. In neighborhood double rows these positions alternate. A $c(2\times4)$ unit cells is indicated in the figure.

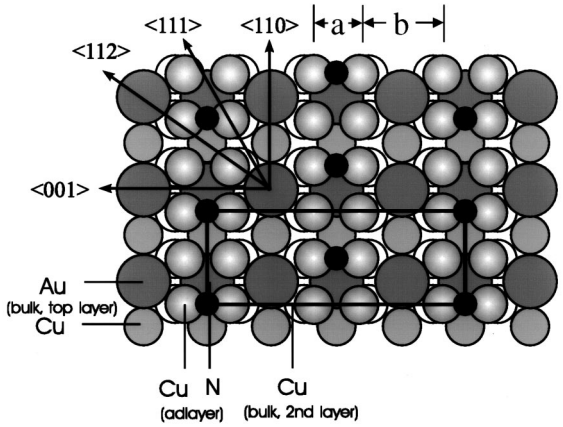

FIG. 6. Model of the nitrogen-covered $Cu_3Au(110)$ surface; a $c(2\times4)$ unit cell and the azimuths discussed in the text are indicated.

In the following we will support the model by our NICISS data. The STM data were used to learn about the topography in the topmost layer; the NICISS data will be used to confirm the chemical identification of the STM atoms, to determine distances in the adlayer and positions of additional atoms above the substrate atoms, and to demonstrate that atom positions in deeper layers are unaffected by the reconstruction.

E. Ion-scattering spectroscopy (NICISS)

A detailed description of the analysis of NICISS scans can be found in Refs. 20 and 21. A quantitative detailed analysis of NICISS data is carried out by comparing the edge slopes of maxima in the experimental NICISS Ψ_{in} scans to the ones obtained by the simulation program FAN.[22] For the simulation we use the model in Fig. 6. Parameters are varied until a good agreement with the experimental results is obtained. The scans will be explained in the following mostly qualitatively, but the model was also quantitatively confirmed.

We begin by comparing the azimuthal scans from the clean and the N covered surfaces. Figure 7 shows azimuthal scans after exposure to nitrogen for the copper signal as well as for the gold signal. The shaded region repeats the azimuthal scan from the clean surface of Fig. 1. Minima for the clean surface are indicated by the solid lines. Apart from a higher background, giving evidence of enhanced surface disorder, there is hardly a difference between the Au scans ob-

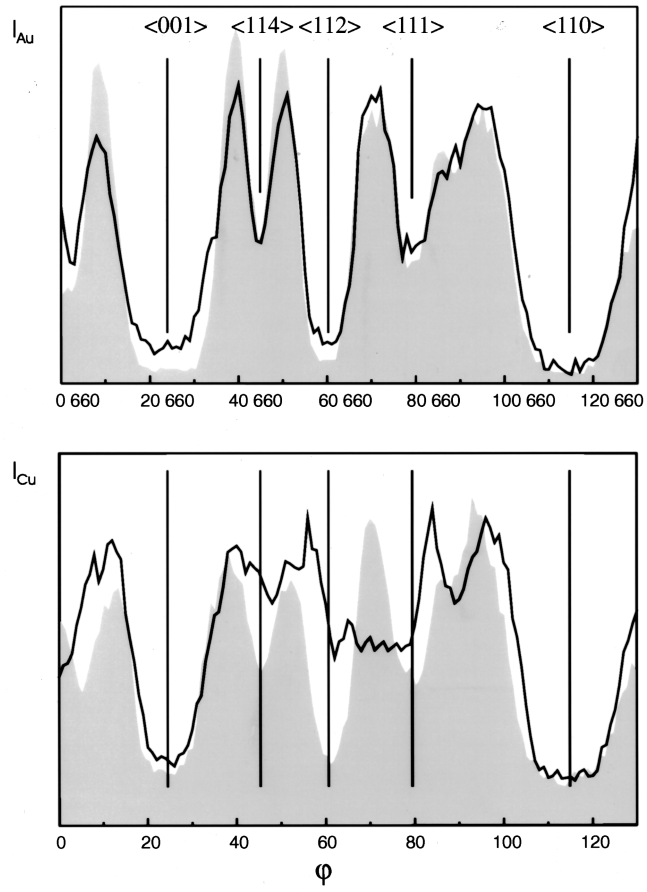

FIG. 7. Azimuthal gold and copper scans (solid lines) after exposure to nitrogen, $\Psi_{in}=4°$; the shaded region represents the φ-scan for the clean surface; solid lines indicate the minima for the clean surface.

tained before and after N exposure. However, for the Cu signal the $\langle 111\rangle$, $\langle 112\rangle$, and $\langle 114\rangle$ azimuths cease to have pronounced minima. In the angular span between $\langle 112\rangle$ and $\langle 111\rangle$ the intensity is about constant at an intermediate level between the maxima and minima appearing in this space for the clean surface. The minimum formerly in $\langle 114\rangle$ is shifted and is not very deep. At $\varphi=89°$, an additional, less deep minimum emerges.

How can this be understood in terms of the suggested structural model? First, the adlayer does not shadow the gold atoms of the former topmost layer; it is similar to the case of the clean surface.[8] Due to the structure of the $Cu_3Au(110)$ surface, the atoms of the second layer are hit by an ion beam even at grazing angle of incidence. The similarity of the Au φ scans before and after nitrogen adsorption is therefore consistent with our model. The changes in the copper polar scans are caused by the in-plane relaxation of the outward segregated additional copper atoms. Cu atoms which were arranged along straight lines with short atomic distances in azimuthal directions between $\langle 001\rangle$ and $\langle 110\rangle$ are now displaced from these directions. The displacement leads to additional short distances in the double rows around 40° and 60° from the $\langle 001\rangle$. These minima are less pronounced because the atomic distances between the double rows are larger.

In the following, we will discuss Ψ_{in} NICISS scans obtained after N adsorption based on Fig. 8. We begin with a qualitative understanding of the Ψ_{in} scans in three azimuthal directions $\langle 001\rangle$, $\langle 110\rangle$, and $\langle 112\rangle$. For $\langle 001\rangle$ and $\langle 112\rangle$ the differences between the scans from the clean and N covered surfaces are large. We then use the understanding of these scans as a guide for parameter variation for the FAN simulation. The shaded regions represent the scan of the clean surface; the solid line, that taken from the nitrogen covered surface. The models represent the two or three parallel cuts in the investigated azimuth perpendicular to the surface that contributes to the scans. The atoms in the (ad)layer are the additional atoms due to nitrogen adsorption. The other layers are numbered according to the clean case.

Edge slopes of the maxima in the NICISS Ψ_{in} scans are related to trajectories in which most of the measured ions and/or atoms are focused on (called main trajectories). They are determined by two atoms, one acting as a focusing atom, the other one as a scattering atom.[19,20] From the position of the steep edges of the maxima in the scans, the relative positions of pairs of atoms in the surface layers can be inferred. The steep edges to be discussed in the following are indicated in the scans, and are numbered from left to right. Corresponding trajectories are indicated in the models; they hit the scattering atom at its center, and touch one or more focusing atoms on the side.

Seen from the $\langle 001\rangle$ azimuth, two Cu distances are observed — a smaller one in the double rows and a larger one between the rows. The resulting Ψ_{in} scan in $\langle 001\rangle$ for copper is shown in Fig. 8(a). The steep edge 2 in the scan appears for the clean surface at $\Psi_{in}=8°$. By nitrogen adsorption the corresponding maxima splits into three maxima that are not distinguishable in the scan, but can be isolated by comparison to the FAN maxima, because FAN simulations are made separately for parallel cuts. The fine line in Fig. 8(a) is the result of the simulation (discussed below) for cut (3). One of the maxima lies clearly to the left, and one to the right of the clean-surface maximum. The third maximum stems from the unaltered trajectory 2 in cut (2). Comparing this to our model, the behavior can be understood by the two distances a and b in the additional layer, with $a<d<b$. The maximum 2 is attenuated because in cut (1) trajectory 2 is blocked by the additional copper. The changes at higher angles can be explained in a similar way.

Figure 8(b) shows the azimuthal scans of the Cu $\langle 110\rangle$ azimuth. In addition to less sharp slopes giving evidence of a higher surface disorder, there are no changes in the steep edges. Ψ_{in} scans for $\langle 001\rangle$ and $\langle 110\rangle$ Au were also analyzed. These scans show also only slight changes with respect to the clean surface scans. These findings are in agreement with the structural model suggested. They also confirm that the atomic positions in the near-surface layers are not affected by the reconstruction.

Figure 8(c) shows the situation for the Au $\langle 112\rangle$ azimuth. There the first maximum 1 is much attenuated, and now seems to consist of a couple of peaks. A glance at the surface model (Fig. 6) clarifies the situation. After nitrogen adsorption the additional copper atoms are located close to the $\langle 112\rangle$ azimuth, but not exactly in line. Ion trajectories are also affected by atoms that are close to the way of the ion without lying in the scattering plane. This can result in a

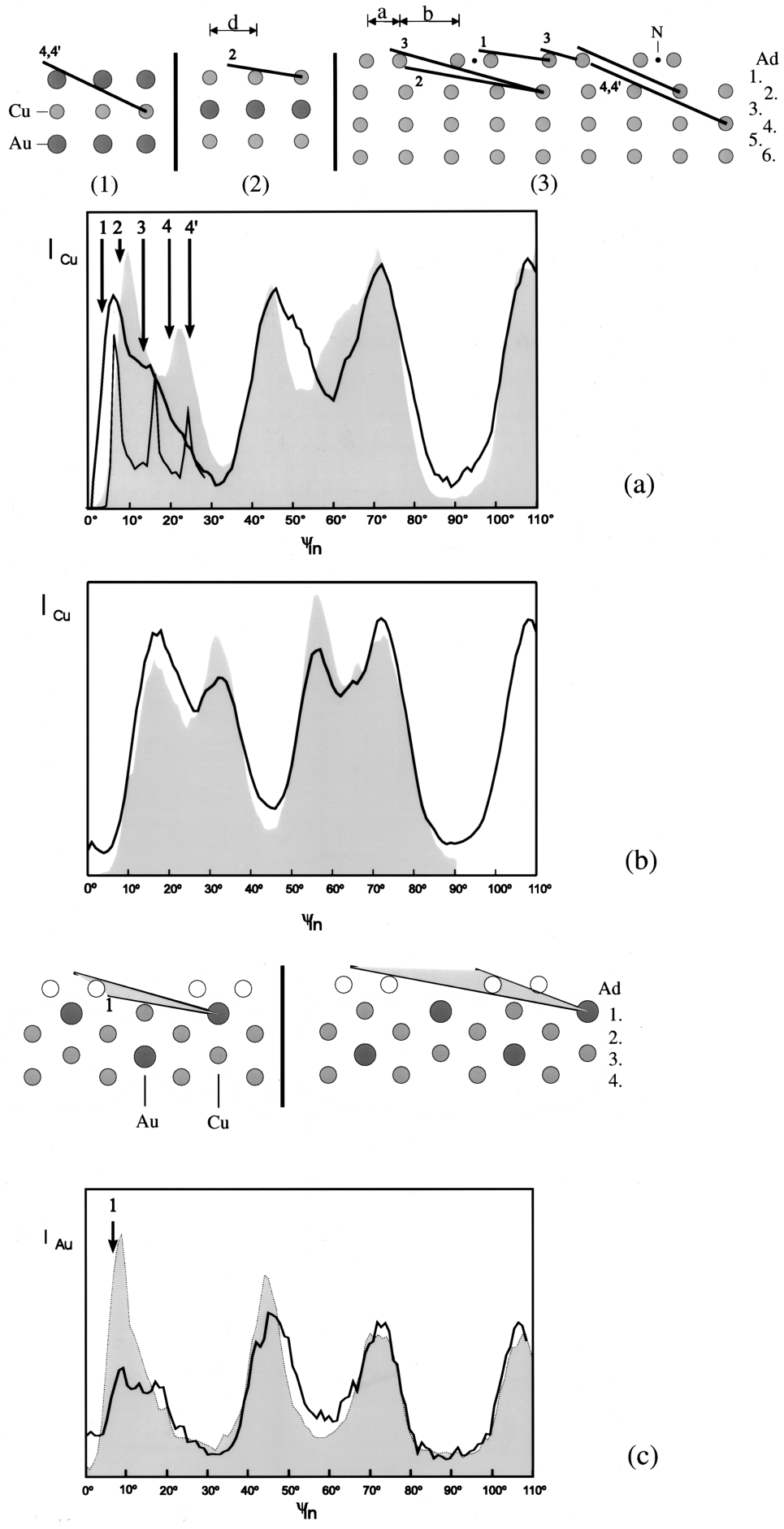

FIG. 8. Polar scans before and after exposure to nitrogen and corresponding crystal cuts. Shaded region before, solid lines after exposure to nitrogen (further details see text). (a) Copper ⟨001⟩ azimuth. (b) Copper ⟨110⟩ azimuth. (b) Gold ⟨112⟩ azimuth.

deflection of the ions out of the plane considered, and therefore in an attenuation of the signal. Similarly an enhancement of the signal by deflection of ions into the plane is possible. Both effects can be seen in the $\langle 112 \rangle$ azimuth. Some of the former trajectories in the $\langle 112 \rangle$ azimuth are attenuated, others become more focused (see the shaded region in the model). This so-called three-dimensional scattering has not been simulated in the FAN program version, but can only be understood qualitatively. We concentrated on scans which are not massively effected by out-of-plane scattering.

A detailed analysis of the relaxation by the FAN simulation can be summarized as follows. The additional peaks at lower incidence angles in the Cu $\langle 001 \rangle$ azimuth can be explained by the in-plane relaxation of the copper rows, and provide information on the distance of the atoms in the additional layer. In a series of FAN simulations, we varied the distances a and b ($a+b=7.5$ Å) and compared the results of the simulations to the experimental steep edges. The Cu distance in $\langle 001 \rangle$ in the bulk is 3.75 Å . We varied the distance in the double rows between $a=2.05$ and 3.75 Å in steps of $\Delta a=0.1$ Å . Hereby the height of the adlayer above the bulk also has to be changed. The bulk distance between layers is 1.33 Å . We varied the distance of the adlayer above the bulk between $z=0.5$ and 2.5 Å in steps of $\Delta z=0.1$. The values for a good agreement between experimental and computational data so obtained are $a=(3.3\pm0.2)$ Å and $z=(0.7\pm0.2)$ Å .

IV. SUMMARY

In conclusion, we were able to characterize the $c(2\times4)$-reconstruction-induced by nitrogen adsorption on the $Cu_3Au(110)$ surface with the combination of STM and NICISS qualitatively as well as quantitatively. The reconstruction consists of additional copper double rows in the $\langle 110 \rangle$ azimuth, with nitrogen atoms in every second bridge position. The nitrogen atoms in neighboring double rows are shifted by one atomic spacing with respect to one another. The in-plane distance of the double rows is $a=(3.3\pm0.2)$ Å . Between the double rows $b=(4.2\pm0.2)$ Å , and with $z=(0.7\pm0.2)$ Å the distances are much closer to the bulk compared to the corresponding bulk interlayer distance.

*Present address: Bayer Ag, Zentrale Forschung TTP4, D-51368 Leverkusen, Germany.

†Present address: Humboldt Universität, ZU Berlin, Institut für Physik, Oberflächen-physik und Atomstoβprozesse, Invalidenstr. 110, D-10115 Berlin, Germany.

[1] R. M. Tromp, E. J. van Loenen, J. E. Demuth, and N. D. Lang, Phys. Rev. B **37**, 9043 (1988).

[2] N. D. Lang, Phys. Rev. Lett. **58**, 45 (1987).

[3] L. Ruan, F. Besenbacher, I. Stensgaard, and E. Laegsgaard, Phys. Rev. Lett. **70**, 4079 (1993).

[4] P. Sautet, J. Dunphy, D. F. Ogletree, C. Joachim, and M. Salmeron, Surf. Sci. **315**, 127 (1994).

[5] H. Niehus, Appl. Phys. A **53**, 388 (1991).

[6] H. Niehus and L. Achete, Surf. Sci. (to be published).

[7] K. H. Besocke, Surf. Sci. **181**, 145 (1987).

[8] H. Niehus, Th. Baumann, M. Voetz, and K. Morgenstern, Surf. Rev. Lett. (to be published).

[9] H. Niehus and C. Achete, Surf. Sci. **289**, 19 (1993).

[10] W. Wallace and G. Ackland, Surf. Sci. Lett. **275**, L685 (1992).

[11] M. Voetz, H. Niehus, J. O'Connor, and G. Comsa, Surf. Sci. **292**, 211 (1993).

[12] R. Spitzl, H. Niehus, and G. Comsa, Surf. Sci. Lett. **250**, L355 (1991).

[13] Y, Kuk, F. M. Chua, P. J. Silverman, and J. A. Meyer, Phys. Rev. B **41**, 122 (1986).

[14] K. Morgenstern, H. Niehus, and G. Comsa, Surf. Sci. **338**, 1 (1995).

[15] In a crude approximation, Rutherford backscattering can be assumed, and the formula can be derived in analogy to J. F. van der Veen, Surf. Sci. Rep. **5**, 199 (1985).

[16] The derivation of S_i is described in Appl. Phys. A **53**, 388 (1991) (Ref. 5).

[17] S. Nakanishi, N. Fukuoka, K. Kawamoto, K. Umezawa, Y. Teraoka, and K. Nakahigashi, Surf. Sci. Lett. **247**, L215 (1991).

[18] S. Nakanishi, K. Kawamoto, N. Fukuoka, and K. Umezawa, Surf. Sci. **261**, 342 (1992).

[19] H. Niehus, R. Spitzl, K. Besocke, and G. Comsa, Phys. Rev. B **43**, 12 619 (1991).

[20] H. Niehus, W. Heiland, and E. Taglauer, Surf. Sci. Rep. **17**, 213 (1993).

[21] H. Niehus, *Practical Surface Analysis, Vol. 2, Ion and Neutral Spectroscopy* (Plenum, New York, 1992), p. 507.

[22] H. Niehus and R. Spitzl, Surf. Inter. Anal. **12**, 287 (1991).